

# Trigermaallene and 1,3-Digermasilaallene

Takeaki Iwamoto, Hidenori Masuda, Chizuko Kabuto, and Mitsuo Kira\*

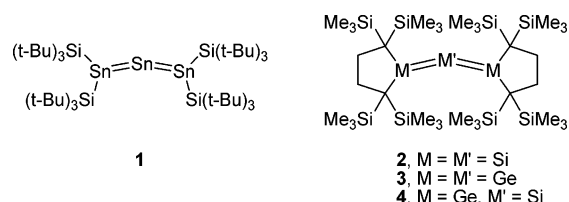
Department of Chemistry, Graduate School of Science, Tohoku University,  
Aoba-ku, Sendai 980-8578, Japan

Received October 21, 2004

**Summary:** X-ray analysis of the first trigermaallene (**3**) and 1,3-digermasilaallene (**4**) revealed that the trimetallaallene skeletons are not linear but significantly bent, similarly to the corresponding trisilaallene **2**. In contrast to **2**, no dynamic disorder was observed for **3** and **4**.

Over the past decade, much attention has been focused on stable cumulative doubly bonded compounds of heavy group 14 elements, due to their unique bonding, structure, and reactivities.<sup>1</sup> Although stable 1-silaallene<sup>2</sup> and related heavy allenes<sup>3</sup> have been isolated and characterized by X-ray crystallography, stable 2-metallaallenes containing a heavy tetravalent dicoordinate ( $\lambda^4\sigma^2$ ) atom have been quite limited. In 1999, Wiberg et al. reported the synthesis and X-ray structure of the marginally stable tristannaallene **1**, which isomerizes to the corresponding cyclotristannene at room temperature.<sup>4</sup> Quite recently, we have synthesized trisilaallene **2** as the first compound containing a  $\lambda^4\sigma^2$  silicon atom.<sup>5,6</sup> In this paper, we report the synthesis and structures of trigermaallene **3** and 1,3-digermasilaallene **4** as the first compounds with cumulative Ge=Ge and Ge=Si double bonds, respectively (Chart 1).<sup>7,8</sup>

Chart 1



A method similar to that used for the synthesis of **2**<sup>5</sup> was applied to the synthesis of trimetallaallenes **3** and **4**. Thus, the reduction using  $\text{KC}_8$  in THF of tetrachlorodigermane **6** and chloro(trichlorosilyl)germane **7**, which were prepared by the insertion of the isolable cyclic germylene **5**<sup>9</sup> into the Si–Cl bond of silicon tetrachloride and Ge–Cl bond of germanium tetrachloride,<sup>10</sup> respectively, gave **3** and **4** in 15% and 24% yields, respectively (Scheme 1). Both **3** and **4** are air-sensitive but thermally stable dark greenish blue crystals (mp: **3**, 197–198 °C; **4**, 211–212 °C dec). The structures of **3** and **4** were determined by <sup>1</sup>H, <sup>13</sup>C, and <sup>29</sup>Si NMR spectroscopy and X-ray crystallography.<sup>11,12</sup>

The molecular structures of **3** and **4** determined by X-ray crystallography at –50 °C are shown in Figures 1 and 2. As single crystals, the 1,3-digermasilaallene **4** has a crystallographic  $C_2$  axis through the central Si atom, while the trigermaallene **3** has no symmetry axis. Similarly to trisilaallene **2** and other known metallaallenes,<sup>3–5</sup> the M–M'–M skeletons in **3** and **4** are not

(8) The syntheses of 1,3-disila-2-gallata- and 2-indataallenic anions have been reported: Nakata, N.; Izumi, R.; Lee, V. Y.; Ichinohe, M.; Sekiguchi, A. *J. Am. Chem. Soc.* **2004**, *126*, 5058.

(9) (a) Kira, M.; Ishida, S.; Iwamoto, T.; Ichinohe, M.; Kabuto, C.; Ignatovich, L.; Sakurai, H. *Chem. Lett.* **1999**, 263. (b) Iwamoto, T.; Masuda, H.; Ishida, S.; Kabuto, C.; Kira, M. *J. Organomet. Chem.* **2004**, *689*, 1337.

(10) Details of the insertion reactions of germylene **5** into M–X bonds (M = Si, Ge; X = Cl, Br) will be reported elsewhere. For the insertion of stable silylenes into Si–Cl bonds, see: (a) Ishida, S.; Iwamoto, T.; Kabuto, C.; Kira, M. *Silicon Chem.* **2003**, *2*, 137. (b) Moser, D. F.; Bosse, T.; Olson, J.; Moser, J. L.; Gusei, I. A.; West, R. *J. Am. Chem. Soc.* **2002**, *124*, 4186.

(11) **3**: dark greenish blue crystals; mp 197–198 °C; <sup>1</sup>H NMR ( $C_6D_6$ ,  $\delta$ ) 0.36 (s, 72H, SiMe<sub>3</sub>), 2.15 (s, 8H, CH<sub>2</sub>); <sup>13</sup>C NMR ( $C_6D_6$ ,  $\delta$ ) 3.5 (SiMe<sub>3</sub>), 36.1 (CH<sub>2</sub>), 42.1 (C); <sup>29</sup>Si NMR ( $C_6D_6$ ,  $\delta$ ) 0.5 (SiMe<sub>3</sub>); UV–vis (hexane;  $\lambda_{max}/nm$  ( $\epsilon$ )) 630 (5300), 496 (2800), 435 (3300), 380 (28 100), 280 (7600, sh). **4**: dark greenish blue crystals; mp 211–212 °C dec; <sup>1</sup>H NMR ( $C_6D_6$ ,  $\delta$ ) 0.36 (s, 72H, SiMe<sub>3</sub>), 2.12 (s, 8H, CH<sub>2</sub>); <sup>13</sup>C NMR ( $C_6D_6$ ,  $\delta$ ) 3.9 (SiMe<sub>3</sub>), 35.9 (CH<sub>2</sub>), 39.1 (C); <sup>29</sup>Si NMR ( $C_6D_6$ ,  $\delta$ ) 1.2 (SiMe<sub>3</sub>), 236.6 (Ge=Si=Ge); UV–vis (hexane;  $\lambda_{max}/nm$  ( $\epsilon$ )) 612 (3100), 488 (2500), 432 (3800), 383 (28 500).

(12) Crystal data for **3** (–50 °C):  $C_{32}H_{80}Si_8Ge_3$ ; fw 907.44; dark greenish blue plate; monoclinic;  $P2_1/n$  (No. 14);  $a = 13.248(6)$  Å;  $b = 17.519(8)$  Å;  $c = 21.316(10)$  Å;  $\beta = 100.609(3)^\circ$ ;  $V = 4882.9(3)$  Å<sup>3</sup>;  $D_{calcd} = 1.234$  g/cm<sup>3</sup>;  $Z = 4$ ;  $R_1 = 0.089$  ( $I > 2\sigma(I)$ );  $wR_2 = 0.189$  (all data); GOF = 1.05. Crystal data for **4** (–50 °C):  $C_{32}H_{80}Si_9Ge_2$ ; fw 862.93; dark greenish blue plate; monoclinic;  $C2/c$  (No. 15);  $a = 24.732(7)$  Å;  $b = 11.512(3)$  Å;  $c = 18.119(6)$  Å;  $\beta = 107.412(1)^\circ$ ;  $V = 4922(3)$  Å<sup>3</sup>;  $D_{calcd} = 1.164$  g/cm<sup>3</sup>;  $Z = 4$ ;  $R_1 = 0.047$  ( $I > 2\sigma(I)$ );  $wR_2 = 0.113$  (all data); GOF = 1.03.

\* To whom correspondence should be addressed. E-mail: mkira@si.chem.tohoku.ac.jp.

(1) Recent review on stable cumulenes of heavy elements: Escudie, J.; Ranaivonjatovo, H.; Rigon, L. *Chem. Rev.* **2000**, *100*, 3639.

(2) (a) Miracle, G. E.; Ball, J. L.; Powell, D. R.; West, R. *J. Am. Chem. Soc.* **1993**, *115*, 11598. (b) Trommer, M.; Miracle, G. E.; Eichler, B. E.; Powell, D. R.; West, R. *Organometallics* **1997**, *16*, 5737. (c) Eichler, B. E.; Miracle, G. E.; Powell, D. R.; West, R. *Main Group Met. Chem.* **1999**, *22*, 147. (d) Ichinohe, M.; Tanaka, T.; Sekiguchi, A. *Chem. Lett.* **2001**, 1074.

(3) Stannaketenimine: (a) Grützmacher, H.; Freitag, S.; Herbst-Irmer, R.; Sheldrick, G. S. *Angew. Chem., Int. Ed. Engl.* **1992**, *31*, 437. 1-Germa-3-phosphaallene: (b) Ramdane, H.; Ranaivonjatovo, H.; Escudie, J.; Mathieu, S.; Knouzi, N. *Organometallics* **1996**, *15*, 3070. (c) El Harouch, Y.; Gornitzka, H.; Ranaivonjatovo, H.; Escudie, J. *J. Organomet. Chem.* **2002**, *643*, 202. 1-Germaallene: (d) Kishikawa, K.; Tokitoh, N.; Okazaki, R. *Organometallics* **1997**, *16*, 5127. (e) Eichler, B. E.; Powell, D. R.; West, R. *Organometallics* **1998**, *17*, 2147 (f) Tokitoh, N.; Kishikawa, K.; Okazaki, R. *Chem. Lett.* **1998**, 811. (g) Eichler, B. E.; Powell, D. R.; West, R. *Organometallics* **1999**, *18*, 540.

(4) Wiberg, N.; Lerner, H.-W.; Vasisht, S.-K.; Wagner, S.; Karaghiosoff, K.; Nöth, H.; Ponikvar, W. *Eur. J. Inorg. Chem.* **1999**, 1211.

(5) Ishida, S.; Iwamoto, T.; Kabuto, C.; Kira, M. *Nature* **2003**, 421, 725.

(6) Very recently, Sekiguchi et al. have reported the synthesis and isolation of the first disilyne: Sekiguchi, A.; Kinjo, R.; Ichinohe, M. *Science* **2004**, *305*, 1755.

(7) For recent reviews of digermenes and germasilenes, see: (a) Driess, M.; Grützmacher, H. *Angew. Chem., Int. Ed. Engl.* **1996**, *35*, 828. (b) Baines, K.; Stibbs, W. G. *Adv. Organomet. Chem.* **1996**, *39*, 275. (c) Power, P. P. *Chem. Rev.* **1999**, *99*, 3463. (d) Escudie, J.; Ranaivonjatovo, H. *Adv. Organomet. Chem.* **1999**, *44*, 113. (e) Weidenbruch, M. *J. Organomet. Chem.* **2002**, *646*, 39. (f) Tokitoh, N.; Okazaki, R. In *The Chemistry of Organic Germanium Tin and Lead Compounds*; Rappoport, Z., Ed.; Wiley: New York, 2002; Vol. 2, Chapter 13, p 843. (g) Lee, V. Y.; Sekiguchi, A. In *The Chemistry of Organic Germanium Tin and Lead Compounds*; Rappoport, Z., Ed.; Wiley: New York, 2002, Vol. 2, Chapter 14, p 903. (h) Sekiguchi, A.; Lee, V. Y. *Chem. Rev.* **2003**, *103*, 1429. (i) Lee, V. Y.; Sekiguchi, A. *Organometallics* **2004**, *23*, 2822.

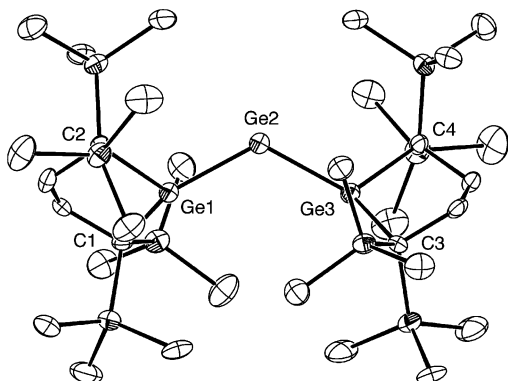


**Figure 1.** Molecular structure of trigermaallene **3** at  $-50$  °C: ORTEP drawing of the whole molecule. Thermal ellipsoids are drawn at the 30% probability level. Hydrogen atoms are omitted for clarity. Selected bond lengths (Å) and angles (deg): Ge1–Ge2 = 2.321(2), Ge2–Ge3 = 2.330(2), Ge1–C1 = 1.994(9), Ge1–C2 = 1.999(8), Ge3–C3 = 1.985(8), Ge3–C4 = 1.999(7); Ge1–Ge2–Ge3 = 122.61(6), Ge2–Ge1–C1 = 137.1(2), Ge2–Ge1–C2 = 115.3(2), C1–Ge1–C2 = 96.2(3), Ge2–Ge3–C3 = 138.0(2), Ge2–Ge3–C4 = 114.5(2), C3–Ge3–C4 = 96.0(3). Distance (Å) between Ge1 and Ge3: 4.080(2). Angle (deg) between the plane (C1–Ge1–C2) and the plane (C3–Ge3–C4): 83.3.

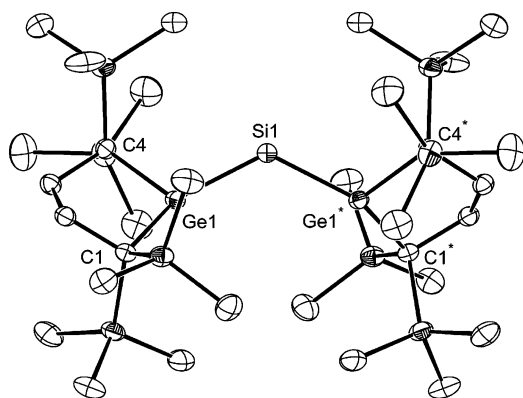
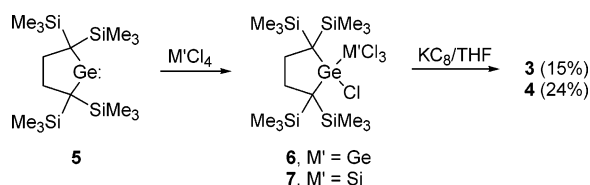


**Figure 2.** Molecular structure of 1,3-digerma-2-silaallene **4** at  $-50$  °C: ORTEP drawing of the whole molecule. Thermal ellipsoids are drawn at the 30% probability level. Hydrogen atoms are omitted for clarity. Selected bond lengths (Å) and angles (deg): Ge1–Si1 = 2.2694(8), Ge1–C1 = 2.007(2), Ge1–C4 = 2.000(3); Ge1–Si1–Ge1\* = 125.71(7), Si1–Ge1–C1 = 138.25(9), Si1–Ge1–C4 = 115.15(9), C1–Ge1–C4 = 95.9(1). Distance (Å) between Ge1 and Ge1\*: 4.039(1). Angle (deg) between the plane (C1–Ge1–C4) and the plane (C1\*–Ge1\*–C4\*): 79.2.

### Scheme 1



linear but significantly bent. The M–M'–M bond angles decreased from  $136.49(6)^\circ$  for **2**<sup>5</sup> to  $125.71(7)^\circ$  for **4** to  $122.61(6)^\circ$  for **3**. Terminal germanium atoms in **3** and **4** adopt a strongly pyramidalized geometry compared to the terminal silicon atoms in **2**; the sums of the bond angles at the Ge1 and Ge3 atoms in **3** and Ge1 (Ge1\*) atom in **4** are 348.6, 348.5, and 349.30°, respectively, which are much smaller than the corresponding values

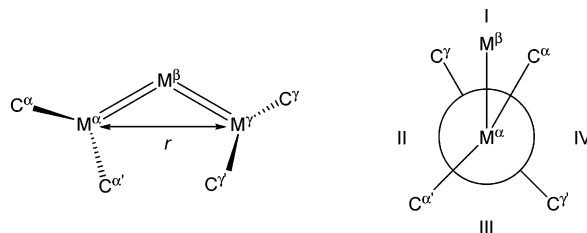


**Figure 3.** (a, left) Atom labeling for the skeleton of trimetallaallenes **2–4**. (b, right) Schematic representation of the trimetallaallene skeleton using a Newman-like projection obtained by looking down the axis through the two terminal atoms  $M^\alpha$  and  $M^\gamma$ . The four quadrants I–IV are defined as shown in the figure. For example, quadrant I is a space divided by  $C^\alpha$ – $M^\alpha$ – $M^\gamma$  and  $M^\alpha$ – $M^\beta$ – $C^\gamma$  planes.

in **2** ( $354.1$  and  $354.9^\circ$ ).<sup>5</sup> The results are consistent with the known tendency that the pyramidalization at germanium atoms in digermenes is larger than that at silicon atoms in the corresponding disilenes.<sup>13</sup> The Ge1–Ge2 and Ge2–Ge3 distances of **3** (2.321(2) and 2.330(3) Å, respectively) are slightly different but in the range of usual Ge=Ge bond lengths (2.21–2.46 Å).<sup>7</sup> The Ge1–Si1 distance of **4** (2.2697(8) Å) is slightly larger than that of a disilagermacyclopentadiene (2.250(1) Å).<sup>14</sup>

To discuss the structural characteristics of trimetallaallenes **2–4** in more detail, we define here the atom labeling and quadrants in the molecules, as shown in Figure 3. Interestingly,  $M^\alpha$ – $M^\gamma$  distances ( $r$ ;  $M = \text{Si}$  for **2** and  $M = \text{Ge}$  for **3** and **4**) are almost constant: 4.054, 4.080, and 4.039 Å for **2–4**, respectively. Furthermore, the shortest intramolecular van der Waals contact in these trimetallaallenes is found between a methyl group in a trimethylsilyl group on  $C^\alpha$  and that on  $C^\gamma$  and the shortest C–C distances found in **2–4** are similar (3.729, 3.863, and 3.710 Å for **2–4**, respectively). The decrease of  $M^\alpha$ – $M^\beta$ – $M^\gamma$  angle with increase of the  $M^\alpha$ – $M^\beta$  (and  $M^\beta$ – $M^\gamma$ ) bond distances from **2** to **3** to **4** is natural if the  $M^\alpha$ – $M^\gamma$  distances are constant.

In a previous paper,<sup>5</sup> we have shown remarkable dynamic disorder of trisilaallene **2** in the solid state; the central silicon atom ( $\text{Si}^\beta$ ) in **2** occupies the four quadrants with different occupancy factors. The behavior is ascribed to the facile intramolecular rotation of  $\text{Si}^\beta$  atom around the  $\text{Si}^\alpha$ – $\text{Si}^\gamma$  axis because of the reversible temperature dependence of the occupancy factors; the energy differences between four rotational isomers are estimated to be less than 1 kcal mol<sup>–1</sup> in the solid state.<sup>5,15</sup> On the other hand, the Ge<sup>β</sup> atom in **3** as well as the Si<sup>β</sup> atom in **4** was observed in only one of the corresponding four quadrants at  $-50$  °C (Figures 1 and 2). The apparent difference in the dynamic behavior between **2** and **3** (and **4**) can be understood from the quite different environmental features of the quadrants between **2** and **3** (and **4**). As shown in Figure 4, the dihedral angles defining the quadrants I–IV are respectively 63.1, 100.9, 95.3, and 100.6° for **3** ( $M = \text{Ge}$ ) and 58.0, 104.7, 92.6, and 104.7° for **4** ( $M = \text{Ge}$ ), while

(13) (a) Goldberg, D. E.; Hitchcock, P. B.; Lappert, M. F.; Thomas, K. M.; Thorne, A.; Fjeldberg, T.; Haaland, A.; Schilling, B. E. R. *J. Chem. Soc., Dalton Trans.* **1986**, 2387. (b) Liang, C.; Allen, L. C. *J. Am. Chem. Soc.* **1990**, *112*, 1039. (c) Trinquier, G.; Malrieu, J.-P. *J. Phys. Chem.* **1990**, *94*, 6184.

(14) Lee, V. Ya.; Ichinohe, M.; Sekiguchi, A. *J. Am. Chem. Soc.* **2000**, *122*, 12604.

(15) The details of the estimation will be reported elsewhere.

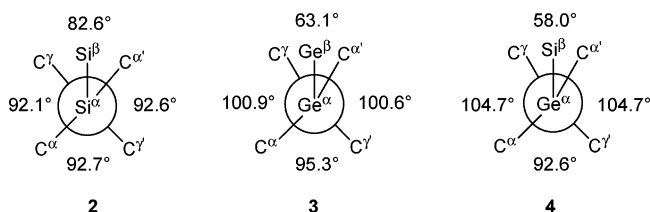
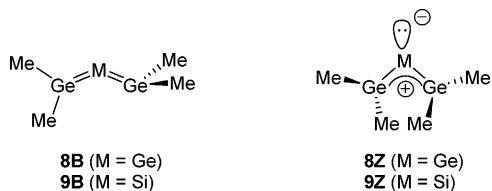


**Figure 4.** Dihedral angles  $C-M^{\alpha}-M^{\gamma}-C$  (deg) defining the four quadrants I–IV for trimetallaallenes **2–4**.

### Chart 2



they are 82.6, 92.1, 92.7, and 92.6° for **2** ( $M = \text{Si}$ ). Since the environments of the four quadrants of **2** are similar with dihedral angles of  $90 \pm 5^\circ$ , the energy differences between the four rotational isomers should be very small. On the other hand, the dihedral angle for quadrant I in **3** (and **4**) is very small compared with those of the other three quadrants. It is suggested that, for **3** and **4**, a rotational isomer having  $M^{\beta}$  in quadrant I is  $>3$  kcal mol $^{-1}$  lower in energy than other isomers that have  $M^{\beta}$  in quadrants II–IV. Apparently, the greater difference in the environments among the four quadrants of **3** (and **4**) as compared to that of **2** can be ascribed to the greater pyramidalization at terminal germanium atoms in **3** and **4**.

Theoretical calculations for tetramethyltrigermaallene (**8**) and tetramethyl-1,3-digermasilaallene (**9**) at the B3LYP/6-31+G(d,p) level<sup>16,17</sup> showed that the optimized structures of **8Z** and **9Z** under constraint of local  $C_2$  symmetry were zwitterionic with very narrow  $\text{Ge}-M-\text{Ge}$  angles ( $87.0^\circ$  for  $M = \text{Ge}$  (**8Z**) and  $88.0^\circ$  for  $M = \text{Si}$  (**9Z**)) and short distances between two terminal Ge atoms (3.250 Å for **8Z** and 3.198 Å for **9Z**) (Chart 2).<sup>18</sup> These structural features in the zwitterionic trimetallaallenes **8Z** and **9Z** are quite similar to those observed for the optimized structure of tetramethyltrisilaallene (**10Z**:  $C_2$  symmetry; Si–Si–Si angle,  $92.4^\circ$ ; distance

(16) Frisch, M. J.; Trucks, G. W.; Schlegel, H. B.; Scuseria, G. E.; Robb, M. A.; Cheeseman, J. R.; Zakrzewski, V. G.; Montgomery, J. A., Jr.; Stratmann, R. E.; Burant, J. C.; Dapprich, S.; Millam, J. M.; Daniels, A. D.; Kudin, K. N.; Strain, M. C.; Farkas, O.; Tomasi, J.; Barone, V.; Cossi, M.; Cammi, R.; Mennucci, B.; Pomelli, C.; Adamo, C.; Clifford, S.; Ochterski, J.; Petersson, G. A.; Ayala, P. Y.; Cui, Q.; Morokuma, K.; Malick, D. K.; Rabuck, A. D.; Raghavachari, K.; Foresman, J. B.; Cioslowski, J.; Ortiz, J. V.; Stefanov, B. B.; Liu, G.; Liashenko, A.; Piskorz, P.; Komaromi, I.; Gomperts, R.; Martin, R. L.; Fox, D. J.; Keith, T.; Al-Laham, M. A.; Peng, C. Y.; Nanayakkara, A.; Gonzalez, C.; Challacombe, M.; Gill, P. M. W.; Johnson, B. G.; Chen, W.; Wong, M. W.; Andres, J. L.; Head-Gordon, M.; Replogle, E. S.; Pople, J. A. *Gaussian 98*, revision A.11.4; Gaussian, Inc.: Pittsburgh, PA, 1998.

(17) See the Supporting Information for the details of the theoretical calculations on **8B**, **8Z**, **9B**, and **9Z**.

(18) When optimization was performed under local  $C_s$  symmetry, each trimetallaallene afforded another type of zwitterionic structure with a narrower  $M-M-M$  bond angle as the energy minimum; the bond angles for the optimized structures **8Z'**–**10Z'** for **8–10**, respectively, are 72.8, 74.3, and  $74.7^\circ$ , respectively. Trimetallaallenes **8Z'** and **9Z'** are 0.9 and 0.6 kcal mol $^{-1}$  lower in energy than **8Z** and **9Z**, respectively, but **10Z'** is 0.3 kcal mol $^{-1}$  higher in energy than **10Z**, respectively. Because the experimentally obtained trimetallaallenes **2–4** have approximately local  $C_2$  symmetry, the data for the zwitterionic trimetallaallenes with local  $C_2$  symmetry are given in the text.

between terminal Si atoms, 3.246 Å). These structural characteristics of **8Z**–**10Z** are quite different from those observed in **3**, **4**, and **2**. Bent allenic structures (**8B** and **9B**) similar to those observed for **3** and **4** were obtained when tetramethyltrimetallaallenes **8** and **9** were optimized under the constraint of the  $\text{Ge}^{\alpha}-\text{Ge}^{\gamma}$  distances fixed to the experimental values (4.080 and 4.039 Å for **3** and **4**, respectively).<sup>19</sup> The structures **8B** and **9B** are 8.4 and 9.8 kcal mol $^{-1}$  higher in energy than **8Z** and **9Z**, respectively. In contrast to rigid and linear carbon allenes, trimetallaallene skeletons are very flexible and are able to be deformed from the intrinsically most stable zwitterionic structures to the bent allenic structures, to avoid the severe steric strains between bulky alkyl substituents, as observed in the structures of **2–4**.

Similarly to **2**,<sup>5</sup> both **3** and **4** showed highly symmetric  $^1\text{H}$ ,  $^{13}\text{C}$ , and  $^{29}\text{Si}$  NMR spectral patterns in solution,<sup>11</sup> suggesting that both **3** and **4** are fluxional in solution with the facile rotation of the central allenic atom around the axis through terminal germanium atoms. Because the  $^1\text{H}$  resonance due to eight trimethylsilyl groups in **3** and **4** remained as a sharp singlet even at  $-80^\circ\text{C}$ , the rotational barrier should be very low. The  $^{29}\text{Si}$  resonance for the central silicon nucleus of **4** appeared at 236.6 ppm, which was much lower than the corresponding resonance for trisilaallene **2** (157 ppm) but was reproduced roughly by the GIAO calculations for **9B** whose skeletal geometry is the same to **4** (272 ppm at the B3LYP/6-311+G(2df,p) level).

UV–vis spectra of **3** and **4** in hexane at room temperature showed five distinct bands ( $\lambda_{\text{max}}/\text{nm}$  ( $\epsilon$ )): 630 (5300), 496 (2800), 435 (3300), 380 (28 100), and 280 (7600, sh) for **3** and 612 (3100), 488 (2500), 432 (3800), 383 (28 500), and 272 (6500) for **4**.<sup>20</sup> The longest absorption bands of **3** and **4** are considerably more red-shifted and more intense than that of **2** ( $\lambda_{\text{max}}$  ( $\epsilon$ ) 584 nm (700)).<sup>5</sup> Less effective  $\pi$  overlaps in  $\text{Ge}=\text{Ge}$  and  $\text{Ge}=\text{Si}$  double bonds of **3** and **4** as compared to that in the  $\text{Si}=\text{Si}$  double bond in **2** could be the reason for the red-shifted intense longest absorption bands of **3** and **4**.

Further investigations are currently in progress.

**Acknowledgment.** This work was supported by the Ministry of Education, Culture, Sports, Science, and Technology of Japan (Grant-in-Aid for Scientific Research on Priority Areas (No. 14078203, “Reaction Control of Dynamic Complexes”).

**Supporting Information Available:** Text, tables, and figures giving details of the synthesis, the X-ray structure determination, and UV–vis spectra of **3** and **4** and optimized coordinates of model compounds and  $\text{Me}_4\text{Ge}_3$  (**8**),  $\text{Me}_4\text{Ge}_2\text{Si}$  (**9**), and  $\text{Me}_3\text{Si}_3$  (**10**); X-ray crystallographic data are also available as CIF files. This material is available free of charge via the Internet at <http://pubs.acs.org>.

OM049183E

(19) It is interesting to note that, under such a constraint, the pyramidalization around terminal germanium atoms and the angle between  $C^{\alpha}-M^{\alpha}-C^{\alpha}$  and  $M^{\alpha}-M^{\beta}-M^{\gamma}$  planes are roughly reproduced. Details of the theoretical calculations will be reported elsewhere.

(20) In a previous paper,<sup>5</sup> only two absorption maxima for **2** were reported at  $\lambda_{\text{max}}/\text{nm}$  ( $\epsilon$ ) 584 (700) and 390 (21 300). In reality, the spectral pattern for **2** is rather similar to those for **3** and **4**; three other bands for **2** are observed as shoulders. See the Supporting Information for details.